IEEE Access
Multidisciplinary | Rapid Review | Open Access Journal

Received January 25, 2018, accepted March 7, 2018, date of publication March 9, 2018, date of current version April 18, 2018.

Digital Object Identifier 10.1109/ACCESS.2018.2814214

A Semidefinite Relaxation Approach to OFDM-IM Detection in Rapidly Time-Varying Channels

JIANPING ZHENG AND HONGMEI LV

State Key Laboratory of Integrated Services Networks, Xidian University, Xi'an, Shaanxi 710071, China

Corresponding author: Jianping Zheng (jpzheng@xidian.edu.cn)

This work was supported by the National Natural Science Foundation of China under Grant 61671340.

ABSTRACT In this paper, the signal detection of orthogonal frequency division multiplexing with index modulation (OFDM-IM) in the rapidly time-varying channel is studied. Due to the inter-carrier interference, the conventional block detectors based on the successive interference cancellation (SIC) strategy, e.g., the signal power (SP) detector, suffer from severe error propagation especially in the case with large normalized Doppler frequency. To address this problem, a semidefinite relaxation (SDR) approach is first proposed. In the proposed SDR detector, the signal feature of OFDM-IM is presented properly as the convex constraints in the SDR programming problem and utilized in the randomization procedure. The SDR detector can avoid the error propagation effectively with a cost of higher polynomial complexity. To reduce the complexity, the group-based SIC-SDR detector is then proposed, where the subcarriers in one OFDM symbol is partitioned into multiple groups, and the SDR detection is performed over each group successively in conjunction with the ordered SIC strategy. However, similar with the SP detector, the SIC-SDR detector also suffers from the error propagation. To boost the performance, we propose to take the solution of the SIC-SDR detector as the initial estimation of a further local search algorithm (LSA). Concretely, after a proper definition of the nearest neighbors of an OFDM-IM signal vector, the proposed combined detector employing the likelihood ascent-search as the LSA is presented. Finally, the validity of the proposed detectors is justified by simulation results, and the combined detector achieves an excellent performance-complexity trade off.

INDEX TERMS *OFDM*, *index modulation*, *semidefinite relaxation*, *likelihood ascent-search*, *successively interference cancellation*, *time-varying channel*.

I. INTRODUCTION

Orthogonal frequency division multiplexing (OFDM) with index modulation (IM) [1]–[3] is a new multi-carrier modulation. The basic idea is that only part of the subcarriers are activated and the activation pattern carries information. By shifting part information from signal constellation to the activation pattern, OFDM-IM shows some advantages in several special scenarios. For example, OFDM-IM shows stronger robustness to the inter-carrier interference (ICI) than the conventional OFDM [3], [4] in the rapidly time-varying (RTV) channel. Due to these potential advantages, OFDM-IM has attracted much attention recently [5]–[26].

These research progresses include the performance analysis in terms of the achievable information rate [5] and the bit error rate (BER) [6], the methods and schemes to improve the error performance [7], to achieve the transmit diversity [8], [9], to achieve higher energy and/or spectral efficiency [10]–[15], to reduce the peak-to-average power ratio [16], and the extensions and variants to the parallel channel [17], the RTV channel [18]–[21], and the MIMO channel [21]–[24]. The interested reader is referred to the recent surveys in [25], [26] for further information.

In this paper, we focus on the study of OFDM-IM in the RTV channel where ICI is severe. In [18], a hybrid IM-OFDM modulation was proposed for the time-varying underwater acoustic (UWA) communication channels. In [19], an ICI self-cancellation scheme was further proposed in the UWA channel. In [20], the linear pre-coding and post-processing matrices at the transceiver were designed to overcome the ICI based on the criterion of maximizing a capacity lower bound. In [21], a circular-shift-based multiple-antenna OFDM-IM scheme was proposed to utilize the antenna diversity and

thereby improve the system performance in the multiple-antenna RTV channel. On the other hand, different from the transmitter design in [18]–[21], several efficient detectors were presented in [3], including the minimum mean square error log-likelihood ratio (MMSE-LLR) detector, the block cancellation (BC) detector based on the successive interference cancellation (SIC) strategy, and the ordered SIC-based signal-power (SP) detector. However, the performance gap of the MMSE-LLR detector from the optimal detector is large, and the BC and SP detectors suffer from the error propagation and show poor performance in the high signal-to-noise ratio (SNR) region especially when the normalized Doppler frequency is large.

Against the above background, the semidefinite relaxation (SDR)-based convex programming [27] is studied here to address the signal detection of OFDM-IM in the RTV channel, since the SDR detector has shown excellent performance in the MIMO system [27]–[32] where the inter-antenna interference exists. In the proposed SDR detector, the character of the OFDM-IM signal is represented properly by some convex constraints in the constrained optimization problem. Moreover, an efficient randomization procedure is presented to acquire the legitimate candidate OFDM-IM vector from the solution of the SDR programming problem. The proposed SDR detector can avoid the error propagation and show much better performance than both the MMSE-LLR and SP detectors, while with a cost of higher polynomial complexity. To reduce the complexity, the SIC strategy is also proposed to employ in the SDR detector. Concretely, the subcarriers in one OFDM symbol is partitioned into multiple groups and the SDR detector is performed successively over each group in conjunction with the ordered SIC. The resulted SIC-SDR detector achieves a complexity reduction with the cost of performance degradation. Furthermore, to boost the performance, we propose to add a second-stage likelihood ascent-search (LAS) algorithm [33] after the SIC-SDR detector. Specifically, the solution of the SIC-SDR detector is employed as the initial estimation of the LAS algorithm. With a proper definition of the nearest neighbors of an OFDM-IM signal vector, the proposed combined LAS with SIC-SDR detector achieves better performance-complexity tradeoff.

The main contributions of this paper can be summarized as follows:

1) The SDR detector is proposed for the OFDM-IM signal detection in the RTV channel. The special signal feature of the IM signal is presented properly as the convex constraint in the convex programming. Furthermore, the low-complexity SIC-SDR detector is also presented.
2) A two-stage detection strategy with the LAS algorithm as the second stage is proposed. To facilitate the LAS implementation, the definition of the nearest neighbors of an OFDM-IM signal vector is presented.
3) Based on the proposed two-stage detection strategy, the combined detector with the low-complexity SIC-SDR or SP detector in the first stage is presented. Moreover, a two-restart combined detector with SP and SIC-SDR as the first-stage detectors, respectively, is also presented.

The rest of the paper is organized as follows. In Section II, the signal model is studied. The proposed SDR and SIC-SDR detectors are presented in Section III. The combined detector with LAS in the second stage is given in Section IV. Simulation results are given in Section V. Finally, Section VI concludes this paper.

Notation: Uppercase boldface letters denote matrices, while lower boldface letters represent vectors. For a matrix $\mathbf{V}$, tr($\mathbf{V}$) and rank($\mathbf{V}$), respectively, denote its trace and rank, diag($\mathbf{V}$) denotes the vector consisting of the diagonal elements of this matrix, and $\mathbf{V} \succeq \mathbf{0}$ presents that it is a semidefinite matrix. The identity matrix is denoted by $\mathbf{I}$. For two vectors $\mathbf{v}_1$ and $\mathbf{v}_2$ with the same size, the operators $\geq$ and $\leq$ are performed element-wisely, and $\mathbf{1}$ denotes the all-one vector. Both the l_2-norm of a vector and the Frobenius norm of a matrix is presented by $||\cdot||$. The notations $(\cdot)^T$ and $(\cdot)^H$ indicate the transpose and Hermitian transpose of a vector or matrix, respectively. Furthermore, $\mathcal{CN}(0, \sigma^2)$ denotes a zero-mean complex Gaussian random variable with variance σ^2, $C(n, k)$ is the binomial coefficient, and $\lfloor\cdot\rfloor$ denotes the floor function. $\mathbb{C}$ and $\mathbb{R}$ represent the complex and real fields, respectively, and for a complex argument, Re{} and Im{} denote the real and imaginary parts, respectively.

II. SIGNAL MODEL

Consider an OFDM symbol with N subcarriers. In OFDM-IM, the N subcarriers are divided into u blocks each with n subcarriers, and the corresponding length-B information bit sequence is partitioned into u blocks each with p bits, i.e., $N = nu$ and $B = pu$. In each block, only n_a out of n subcarriers are activated to transmit signals, and the other $n - n_a$ subcarriers remain silent. The first p_1 bits of the incoming p-bit sequence are used to determine the indices of the n_a activated subcarriers and remaining p_2 ($p_2 = p - p_1$) bits are mapped into the n_a M-ary QAM/PSK constellation points. Obviously, it has $p_1 = \lfloor \log_2(C(n, n_a)) \rfloor$ and $p_2 = n_a \log_2 M$.

Consider the IM signal in the β-th, $\beta = 1, 2, ..., u$ block. The set of the indices of the active subcarriers is denoted by

$$I_\beta = \left\{ i_{\beta,1}, i_{\beta,2}, ..., i_{\beta,n_a} \right\} \tag{1}$$

with $i_{\beta,\gamma} \in \{1, 2, ..., n\}$, $\gamma = 1, 2, ..., n_a$. Correspondingly, the set of the n_a QAM/PSK symbols modulated over these active subcarriers is denoted by

$$S_\beta = \left\{ s_{\beta,1}, s_{\beta,2}, ..., s_{\beta,n_a} \right\} \tag{2}$$

where $s_{\beta,\gamma} \in \mathcal{S}$, $\gamma = 1, 2, \cdots n_a$ and $\mathcal{S}$ is the QAM/PSK constellation. Then, the frequency-domain (FD) signal in this block can be expressed by

$$\mathbf{x}_\beta = \sum_{\gamma=1}^{n_a} s_{\beta,\gamma} \mathbf{e}_{i_{\beta,\gamma}} \tag{3}$$

where $\mathbf{e}_{i_{\beta,\gamma}}$ is the n-dimensional all-zero vector except a one in position $i_{\beta,\gamma}$.

Concatenating the u IM blocks, the FD signal in one OFDM symbol can be expressed by

$$\mathbf{x} = \left[\mathbf{x}_1^T, \mathbf{x}_2^T, \ldots, \mathbf{x}_u^T\right]^T \tag{4}$$

The FD signal $\mathbf{x}$ is further transformed into the time-domain by

$$\mathbf{x}' = \frac{1}{\sqrt{K}}\mathbf{W}_N^H\mathbf{x} \tag{5}$$

where $\mathbf{W}_N$ is the fast Fourier transform (FFT) matrix with $\mathbf{W}_N^H\mathbf{W}_N = N\mathbf{I}_N$. After adding a length-$L$ cyclic prefix (CP), the signal is transmitted over doubly selective fading channels.

At the receiver, after removing the CP and performing the inverse FFT (IFFT), the received FD signal can be expressed by

$$\mathbf{y} = \mathbf{G}\mathbf{x} + \boldsymbol{\omega} \tag{6}$$

where $\mathbf{y} = [y_1, y_2, \ldots, y_N]^T \in \mathbb{C}^{N\times 1}$ and $\mathbf{G} = \mathbf{W}_N\mathbf{R}_{CP}\mathbf{H}\mathbf{T}_{CP}\mathbf{W}_N^H \in \mathbb{C}^{N\times N}$. Here, $\mathbf{T}_{CP} \triangleq \left[\mathbf{I}_{CP}^T\mathbf{I}_N\right]^T$ is the $(N+L)\times N$ matrix that inserts the CP with $\mathbf{I}_{CP}$ consisting of the last L rows of the identity matrix $\mathbf{I}_N$, $\mathbf{R}_{CP} \triangleq [\mathbf{0}_{N\times L}\mathbf{I}_N]$ is the $N\times(N+L)$ matrix that removes CP, $\boldsymbol{\omega} \sim \mathcal{CN}(0, N_{0,F})$ is the FD noise, and $\mathbf{H} \in \mathbb{C}^{(N+L)\times(N+L)}$ is the time domain channel matrix.

In the RTV channel, the equivalent FD channel matrix $\mathbf{G}$ is general non-diagonal, thus the optimal maximum-likelihood (ML) detection, described by

$$\hat{\mathbf{x}} = \underset{\mathbf{x}}{\operatorname{argmin}} \|\mathbf{y} - \mathbf{G}\mathbf{x}\|^2 \tag{7}$$

is prohibitively complex. To reduce the complexity, the MMSE-LLR detector and the ordered SIC-based SP detector are proposed in [3]. However, in the scenario with large normalized Doppler frequency, the SP detector suffers from a severe error propagation and has poor performance in high SNR regions, and the MMSE-LLR detection shows a large performance gap from the ML detection. In the next section, the SDR detector is proposed to achieve better performance in the overall SNR region.

III. PROPOSED SDR DETECTOR

A. OPTIMIZATION PROBLEM FORMULATION

To derive the SDR detector, we first transfer the signal model in (6) into the real filed by

$$\begin{aligned}\bar{\mathbf{x}} &:= \left[\mathrm{Re}\{\mathbf{x}\}^T\ \mathrm{Im}\{\mathbf{x}\}^T\right]^T\\ \bar{\mathbf{G}} &:= \begin{bmatrix}\mathrm{Re}\{\mathbf{G}\} & -\mathrm{Im}\{\mathbf{G}\}\\ \mathrm{Im}\{\mathbf{G}\} & \mathrm{Re}\{\mathbf{G}\}\end{bmatrix}\\ \bar{\mathbf{y}} &:= \left[\mathrm{Re}\{\mathbf{y}\}^T\ \mathrm{Im}\{\mathbf{y}\}^T\right]^T\end{aligned} \tag{8}$$

Then, the optimal ML detection problem can be expressed by the following constrained optimization problem

$$\mathbf{OP1}: \begin{cases}\min\limits_{\bar{\mathbf{x}}} \left\|\bar{\mathbf{y}} - \bar{\mathbf{G}}\bar{\mathbf{x}}\right\|^2\\ s.t.\ \bar{\mathbf{x}} \text{ is an OFDM - IM singal (C1)}\end{cases} \tag{9}$$

The objective function in OP1 can be computed explicitly by

$$\left\|\bar{\mathbf{y}} - \bar{\mathbf{G}}\bar{\mathbf{x}}\right\|^2 = \bar{\mathbf{x}}^T\bar{\mathbf{G}}^T\bar{\mathbf{G}}\bar{\mathbf{x}} - 2\bar{\mathbf{y}}^T\bar{\mathbf{G}}\bar{\mathbf{x}} + \bar{\mathbf{y}}^T\bar{\mathbf{y}} \tag{10}$$

Ignoring the constant term with respect to $\bar{\mathbf{x}}$, OP1 can be rewritten as

$$\mathbf{OP1}': \begin{cases}\min\limits_{\bar{\mathbf{x}}} \bar{\mathbf{x}}^T\bar{\mathbf{G}}^T\bar{\mathbf{G}}\bar{\mathbf{x}} - 2\bar{\mathbf{y}}^T\bar{\mathbf{G}}\bar{\mathbf{x}}\\ s.t.\ \bar{\mathbf{x}} \text{ is an OFDM - IM singal (C1)}\end{cases} \tag{11}$$

Define $\mathbf{z} = \left[\bar{\mathbf{x}}^T\ 1\right]^T \in \mathbb{R}^{2N+1}$, and

$$\mathbf{Q} = \begin{bmatrix}\bar{\mathbf{G}}^T\bar{\mathbf{G}} & -\bar{\mathbf{y}}^T\bar{\mathbf{G}}\\ -\bar{\mathbf{G}}^T\bar{\mathbf{y}} & \mathbf{0}\end{bmatrix} \tag{12}$$

Then, OP1′ can be reformulated by

$$\mathbf{OP1}'': \begin{cases}\min\limits_{\mathbf{z}} \mathbf{z}^T\mathbf{Q}\mathbf{z}\\ s.t.:\ \mathbf{z}_{1:2N} \text{ is an OFDM - IM singal (C1')}\\ \qquad z_{2N+1} = 1\end{cases} \tag{13}$$

Define $\mathbf{Z} = \mathbf{z}\mathbf{z}^T$, and partition it by

$$\mathbf{Z} = \begin{bmatrix}\mathbf{Z}_{1,1} & \mathbf{Z}_{1,2}\\ \mathbf{Z}_{1,2}^T & \mathbf{Z}_{2,2}\end{bmatrix} = \begin{bmatrix}\bar{\mathbf{x}}\bar{\mathbf{x}}^T & \bar{\mathbf{x}}\\ \bar{\mathbf{x}}^T & 1\end{bmatrix} \tag{14}$$

with $\mathbf{Z}_{1,1} = \bar{\mathbf{x}}\bar{\mathbf{x}}^T$, $\mathbf{Z}_{1,2} = \bar{\mathbf{x}}$ and $\mathbf{Z}_{2,2} = 1$. Noting that $\mathbf{z}^T\mathbf{Q}\mathbf{z} = \mathrm{tr}(\mathbf{z}^T\mathbf{Q}\mathbf{z}) = \mathrm{tr}(\mathbf{Q}\mathbf{z}\mathbf{z}^T) = \mathrm{tr}(\mathbf{Q}\mathbf{Z})$, OP1″ can be further expressed by

$$\mathbf{OP1}''': \begin{cases}\min\limits_{\mathbf{Z}} \mathrm{tr}\,(\mathbf{Q}\mathbf{Z})\\ s.t.:\ \mathbf{Z} = \mathbf{z}\mathbf{z}^T = \begin{bmatrix}\mathbf{Z}_{1,1} & \mathbf{Z}_{1,2}\\ \mathbf{Z}_{1,2}^T & \mathbf{Z}_{2,2}\end{bmatrix} \text{ (C2)}\\ \qquad \mathbf{z}_{1:2N} \text{ is an OFDM - IM singal (C1')}\\ \qquad \mathbf{Z}_{2,2} = 1\end{cases} \tag{15}$$

B. RELAXATION

The problem OP1‴ is not convex, since the constraints C1' and C2 are non-convex. To make it be convex, the relaxation of both the constraints are given in the following.

First, note that the FD signal in OFDM-IM is zero (silent subcarrier) or from $\mathcal{S}$ (active subcarrier). Denote $\Re$ and $\Im$, respectively, as the set of real and imaginary parts of the signal points in the constellation $\mathcal{S}$. For example, for the QPSK signal constellation $\mathcal{S} = \{\pm 1 \pm j\}$ with j being the imaginary unit, i.e., $j = \sqrt{-1}$, it has $\Re = \Im = \{\pm 1\}$. Define $\mathcal{Z}_1 \triangleq \Re \cup \{0\}$, $\mathcal{Z}_2 \triangleq \Im \cup \{0\}$. Then, it has

$$z_i \in \begin{cases}\mathcal{Z}_1, & bi = 1, \ldots, N,\\ \mathcal{Z}_2, & i = N+1, \ldots, 2N\end{cases} \text{ (C1 - 1)} \tag{16}$$

Furthermore, the constraint C1-1 can be explicitly presented by a set of inequalities by extending the method in [28].

Example 1: Consider the 16-QAM signal constellation $\mathcal{S} = \{a + bj, a, b \in \{\pm 1, \pm 3\}\}$. Define the continued real-valued intervals $\Omega_1 := [-3, 3]$, $\Omega_2 := (-3, -1)$, $\Omega_3 := (-1, 0)$, $\Omega_4 := (0, 1)$, $\Omega_5 := (1, 3)$. The set $\mathcal{Z}_1 = \mathcal{Z}_2 = \mathcal{Z} = \{0, \pm 1, \pm 3\}$ can be presented alternatively by

$$\mathcal{Z} = \Omega_1 \cap \bar{\Omega}_2 \cap \bar{\Omega}_3 \cap \bar{\Omega}_4 \cap \bar{\Omega}_5 \tag{17}$$

where $\bar{\Omega}_i$ is the complementary set of Ω_i for $i = 2, \ldots, 5$. Then, the constraint C1-1 can be reformulated by the following inequality set

$$\begin{aligned} 0 \le {z_i}^2 &\le 9 \\ {z_i}^2 + 4z_i + 3 &\ge 0 \\ {z_i}^2 + z_i &\ge 0 \\ {z_i}^2 - z_i &\ge 0 \\ {z_i}^2 - 4z_i + 3 &\ge 0 \end{aligned} \tag{18}$$

for $i = 1, \ldots, 2N$. Recalling the matrix partition of $\mathbf{Z}$ in (14), we get

$$\begin{aligned} \mathbf{0} \le \mathrm{diag}(\mathbf{Z}_{1,1}) &\le 9\mathbf{1} \\ \mathrm{diag}(\mathbf{Z}_{1,1}) + 4\mathbf{Z}_{1,2} + 3\mathbf{1} &\ge \mathbf{0} \\ \mathrm{diag}(\mathbf{Z}_{1,1}) + \mathbf{Z}_{1,2} &\ge \mathbf{0} \\ \mathrm{diag}(\mathbf{Z}_{1,1}) - \mathbf{Z}_{1,2} &\ge \mathbf{0} \\ \mathrm{diag}(\mathbf{Z}_{1,1}) - 4\mathbf{Z}_{1,2} + 3\mathbf{1} &\ge \mathbf{0} \end{aligned} \tag{19}$$

Second, consider the constraint that only n_a subcarriers are active in one IM block. Denote $\mathbf{Z}^b_{1,1}, b = 1, \ldots, 2u$ as the b-th submatrix of size $n \times n$ along the main diagonal of the matrix $\mathbf{Z}_{1,1}$. Then, from (8) and (14), $\mathrm{diag}\left(\mathbf{Z}^b_{1,1}\right)$ presents the squared value of the real part of the b-th IM block if $b \le u$, and that of the imaginary part, otherwise. Define the squared minimum and maximum values of $\Re$ and $\Im$ by

$$\begin{aligned} v_{r,1} &= \min_{s \in \Re} s^2, \quad v_{r,2} = \max_{s \in \Re} s^2 \\ v_{i,1} &= \min_{s \in \Im} s^2, \quad v_{i,2} = \max_{s \in \Im} s^2 \end{aligned} \tag{20}$$

Then, the constraint that only n_a subcarriers are active can be approximated by

$$\begin{cases} n_a v_{r,1} \le \mathrm{tr}\left\{\mathbf{Z}^b_{1,1}\right\} \le n_a v_{r,2}, & b = 1, \ldots, u \\ n_a v_{i,1} \le \mathrm{tr}\left\{\mathbf{Z}^b_{1,1}\right\} \le n_a v_{i,2}, & b = u+1, \ldots, 2u \end{cases} \quad \text{(C1 - 2)} \tag{21}$$

Third, the constraint C2 can be presented by

$$\mathbf{Z} \succeq \mathbf{0}, \quad \mathrm{rank}\,(\mathbf{Z}) = 1 \text{ (C2')} \tag{22}$$

The rank-1 constraint in C2' is non-convex, and is usually ignored in the SDR-based convex programming.

Finally, the optimization problem OP1‴ can be approximated by

$$\mathbf{OP2}: \begin{cases} \min\limits_{\mathbf{Z}} \ \mathrm{tr}\,(\mathbf{QZ}) \\ s.t.: \ \mathrm{C1-1}, \ \mathrm{C1-2} \\ \qquad \mathbf{Z} \succeq \mathbf{0} \\ \qquad \mathbf{Z}_{2,2} = 1 \end{cases} \tag{23}$$

With the inequality set presentation of C1-1, like (19) for 16-QAM, OP2 becomes a convex optimization problem. To solve OP2, we used CVX, a package for specifying and solving convex programs [34], [35].

Example 1 (continued): For the 16-QAM constellation, from (20), it has $v_{r,1} = v_{i,1} = 1, v_{r,2} = v_{i,2} = 9$, and OP2 can be explicitly expressed by the convex optimization problem:

OP2 for 16-QAM:

$$\begin{cases} \min\limits_{\mathbf{Z}} \ \mathrm{Tr}\,(\mathbf{QZ}) \\ s.t.: \ \mathbf{0} \le \mathrm{diag}(\mathbf{Z}_{1,1}) \le 9\mathbf{1} \\ \qquad \mathrm{diag}(\mathbf{Z}_{1,1}) + 4\mathbf{Z}_{1,2} + 3\mathbf{1} \ge \mathbf{0} \\ \qquad \mathrm{diag}(\mathbf{Z}_{1,1}) + \mathbf{Z}_{1,2} \ge \mathbf{0} \\ \qquad \mathrm{diag}(\mathbf{Z}_{1,1}) - \mathbf{Z}_{1,2} \ge \mathbf{0} \\ \qquad \mathrm{diag}(\mathbf{Z}_{1,1}) - 4\mathbf{Z}_{1,2} + 3\mathbf{1} \ge \mathbf{0} \\ \qquad n_a \le \mathrm{tr}\left\{\mathbf{Z}^b_{1,1}\right\} \le n_a 9, \quad b = 1, \ldots, 2u \\ \qquad \mathbf{Z} \succ= \mathbf{0} \\ \qquad \mathbf{Z}_{2,2} = 1 \end{cases} \tag{24}$$

C. RANDOMIZATION

Denote $\hat{\mathbf{Z}}$ as the solution of OP2. The following randomization procedure is performed to obtain the estimation of $\mathbf{x}$. First, perform the Cholesky factorization $\hat{\mathbf{Z}} = \mathbf{V}\mathbf{V}^T$, and generate L_r random vectors $\mathbf{u}_l$, $l = 1, \ldots, L_r$, from the uniform distribution on the unit sphere independently. Next, compute the candidate vectors by

$$\tilde{\mathbf{x}} = \frac{\mathbf{V}\mathbf{u}_l}{\mathbf{v}_{2N+1}\mathbf{u}_l}, \quad l = 1, \ldots, L_r \tag{25}$$

where $\mathbf{v}_{2N+1}$ denotes the last row of $\mathbf{V}$. Then, $\mathbf{x}$ can be recovered through the following steps.

1) Reconstruct the signal vector $\tilde{\mathbf{x}}_l$ in the complex field so that
$$\tilde{\mathbf{x}} = \left[\mathrm{Re}\{\tilde{\mathbf{x}}_l\}^T \ \mathrm{Im}\{\tilde{\mathbf{x}}_l\}^T\right]^T, \quad l = 1, \ldots, L_r \tag{26}$$
2) Partition $\tilde{\mathbf{x}}_l, l = 1, \ldots, L_r$ by $\tilde{\mathbf{x}}_l = \left[\tilde{\mathbf{x}}^T_{l,1}, \ldots, \tilde{\mathbf{x}}^T_{l,u}\right]^T$ with $\tilde{\mathbf{x}}^T_{l,b} \in \mathbb{C}^n, b = 1, \ldots, u$.
3) For each candidate $l = 1, \ldots, L_r$ and each block b, $b = 1, \ldots, u$, obtain $\tilde{\mathbf{x}}^q_{l,b} = \mathit{Quant}\left(\tilde{\mathbf{x}}_{l,b}\right)$ through the element-wise constellation quantization, i.e., quantize each element of $\tilde{\mathbf{x}}_{l,b}$ to the nearest point of

the signal constellation $\mathcal{S}$. Moreover, compute the metrics

$$\Gamma_{l,b,t} = \left|\tilde{\mathbf{x}}_{l,b}(t)\right|^2 - \left|\tilde{\mathbf{x}}_{l,b}(t) - \tilde{\mathbf{x}}^q_{l,b}(t)\right|^2, \quad t = 1, \ldots, n \tag{27}$$

4) Find out the n_a indices with the largest metrics in the set $\{\Gamma_{l,b,t}\}_{t=1,\ldots,n}$, and denoted them as $t_1, \ldots, t_{n_a}$. Obtain the legitimate candidate signal vector $\hat{\mathbf{x}}_{l,b}$, $l = 1, \ldots, L_r$, $b = 1, \ldots, u$ by

$$\hat{\mathbf{x}}_{l,b}(t) = \begin{cases} \tilde{\mathbf{x}}^q_{l,b}(t), & \text{if } t \in \{t_1, \ldots, t_{n_a}\} \\ 0, & \text{otherwise} \end{cases} \tag{28}$$

5) The signal $\mathbf{x}$ is recovered by

$$\hat{\mathbf{x}} = \underset{\mathbf{x} \in \{\hat{\mathbf{x}}_1, \ldots, \hat{\mathbf{x}}_{L_r}\}}{\arg\min} \|\mathbf{y} - \mathbf{G}\mathbf{x}\|^2 \tag{29}$$

Remark: The idea behind Steps 3) and 4) is interpreted as follows. The log-likelihood ratio (LLR) of the probability of the $((b-1)n+t)$-th subcarrier associated with $\tilde{\mathbf{x}}_{l,b}(t)$ being active to that of being silent can be computed by

$$\begin{aligned} \mathrm{LLR}_{l,b,t} &= \ln \frac{p\left(y_{(b-1)n+t} | \hat{\mathbf{x}}_{l,b}(t) \neq 0\right)}{p\left(y_{(b-1)n+t} | \hat{\mathbf{x}}_{l,b}(t) = 0\right)} + \mathrm{LLR}^{ap}_{b,t} \\ &\approx \ln \frac{p(\tilde{\mathbf{x}}_{l,b}(t)) | \hat{\mathbf{x}}_{l,b}(t) = \tilde{\mathbf{x}}^q_{l,b}(t))}{p(\tilde{\mathbf{x}}_{l,b}(t) | \hat{\mathbf{x}}_{l,b}(t) = 0)} + \mathrm{LLR}^{ap}_{b,t} \\ &= \frac{\left|\tilde{\mathbf{x}}_{l,b}(t)\right|^2 - \left|\tilde{\mathbf{x}}_{l,b}(t) - \tilde{\mathbf{x}}^q_{l,b}(t)\right|^2}{N_{0,F}} + \mathrm{LLR}^{ap}_{b,t} \\ &= \frac{1}{N_{0,F}} \Gamma_{l,b,t} + \mathrm{LLR}^{ap}_{b,t}, \quad t = 1, 2, \ldots, n \end{aligned} \tag{30}$$

where $\mathrm{LLR}^{ap}_{b,t}$ presents the *a priori* LLR information of this subcarrier and is the same for all $b = 1, \ldots, u$ and $t = 1, \ldots, n$. Therefore, as given in (28), the subcarriers with the largest metrics defined by (27) are determined to be active.

D. SIC-SDR

It is well known that the complexity of the SDR detector is $\mathcal{O}\left(N^{3.5}\right)$ [27], which is still very high especially for large N. To reduce the complexity, the ordered SIC detection strategy can be utilized, and the the resulted detector is abbreviated as SIC-SDR.

The subcarriers in one OFDM symbol are partitioned into K groups, each consisting of $N_0 = N/K$ adjacent subcarriers. Here, we assume N_0/n is an integer. Then, (6) can be rewritten as

$$\begin{pmatrix} \mathbf{y}^1 \\ \mathbf{y}^2 \\ \vdots \\ \mathbf{y}^K \end{pmatrix} = \begin{pmatrix} \mathbf{G}^{1,1} & \mathbf{G}^{1,2} & \cdots & \mathbf{G}^{1,K} \\ \mathbf{G}^{2,1} & \mathbf{G}^{2,1} & \cdots & \mathbf{G}^{2,K} \\ \vdots & \vdots & \ddots & \vdots \\ \mathbf{G}^{K,1} & \mathbf{G}^{K,1} & \cdots & \mathbf{G}^{K,K} \end{pmatrix} \begin{pmatrix} \mathbf{x}^1 \\ \mathbf{x}^2 \\ \vdots \\ \mathbf{x}^K \end{pmatrix} + \begin{pmatrix} \boldsymbol{\omega}^1 \\ \boldsymbol{\omega}^2 \\ \vdots \\ \boldsymbol{\omega}^K \end{pmatrix} \tag{31}$$

Here, $\mathbf{G}^{i,j} \in \mathbb{C}^{N_0 \times N_0}$, $i, j = 1, \ldots, K$ is the (i,j)-th subblock of $\mathbf{G}$, and $\mathbf{x}^i, \mathbf{y}^i, \boldsymbol{\omega}^i \in \mathbb{C}^{N_0}$, $i = 1, \ldots, K$ are the i-th subblock of $\mathbf{x}$, $\mathbf{y}$, and $\boldsymbol{\omega}$, respectively.

The SIC-SDR detector first orders the K groups according to their signal powers defined as $\left\|\mathbf{G}^{k,k}\right\|^2$, $k = 1, \ldots, K$. Then, the SDR is performed successively from the group with the largest power to that with the least, in conjunction with the SIC. Without loss of generality, assume $\left\|\mathbf{G}^{1,1}\right\|^2 \geq \left\|\mathbf{G}^{2,2}\right\|^2 \geq \cdots \geq \left\|\mathbf{G}^{K,K}\right\|^2$. The signal detector for the k-th, $k = 1, \ldots, K$ group can be described explicitly as follows.

The interferences from the first $k-1$ estimated signals $\hat{\mathbf{x}}^i$, $i = 1, \ldots, k-1$ are first cancelled by

$$\mathbf{y}^k = \mathbf{y}^k - \sum_{i=1}^{k-1} \mathbf{G}^{k,i} \hat{\mathbf{x}}^i \tag{32}$$

With the assumption of $\mathbf{x}^i = \hat{\mathbf{x}}^i$, $i = 1, \ldots, k-1$, (32) can be further presented as

$$\mathbf{y}^k = \mathbf{G}^{k,k}\mathbf{x}^k + \sum_{i=k+1}^{K} \mathbf{G}^{k,i}\mathbf{x}^i + \boldsymbol{\omega}^k \tag{33}$$

The second term on the right hand side of (33) is the ICI from the undetected groups, and is viewed as noise in the SDR detection for $\mathbf{x}^k$.

The SIC-SDR detector is summarized in Algorithm 1. It is easy to see that its complexity is $\mathcal{O}\left(K(N/K)^{3.5}\right)$.

Algorithm 1 SIC-SDR Detector

1. Order the K groups according to their signal powers.
2. Assume $\left\|\mathbf{G}^{1,1}\right\|^2 \geq \left\|\mathbf{G}^{2,2}\right\|^2 \geq \cdots \geq \left\|\mathbf{G}^{K,K}\right\|^2$.
3. Set $k = 1$
4. **while** $(k \leq K)$:
5. Obtain the estimation $\hat{\mathbf{x}}^k$ by using the SDR detector
6. over the signal model (33).
7. $k \leftarrow k + 1$
8. If $k \leq K$, update $\mathbf{y}^k$ by (32).
9. **end while**

IV. COMBINED WITH LAS ALGORITHM

In Section III-D, the proposed SIC-SDR detector achieves a complexity reduction with the cost of performance degradation. To boost the performance, we propose to introduce a post-processing procedure, e.g., the local search algorithm. Concretely, the estimation obtained by SIC-SDR is employed as the initial vector of the LAS algorithm [33], as shown in Fig. 1(*a*).

The main challenging in the employing of the LAS algorithm in the OFDM-IM detection is how to define the neighbor vector. Different from the conventional MIMO or OFDM signal, where the nearest neighbor can be defined as the vector with only one entry changing to its nearest constellation point [33], the definition of nearest neighbor is more difficult due to the special signal character of OFDM-IM. Define the activation pattern (AP) as the n-dimensional vector with

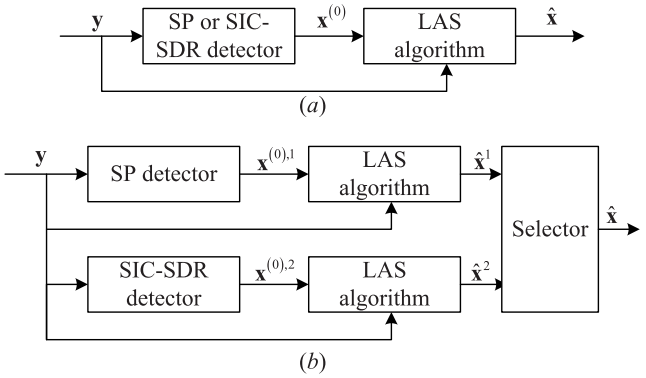

FIGURE 1. The proposed (*a*) combined detector with the low-complexity SP or SIC-SDR detector in the first stage and the LAS algorithm as the second stage, and (*b*) the two-restart combined detector with the SP and SIC-SDR detectors, respectively, as the first stage detector in the parallel processing.

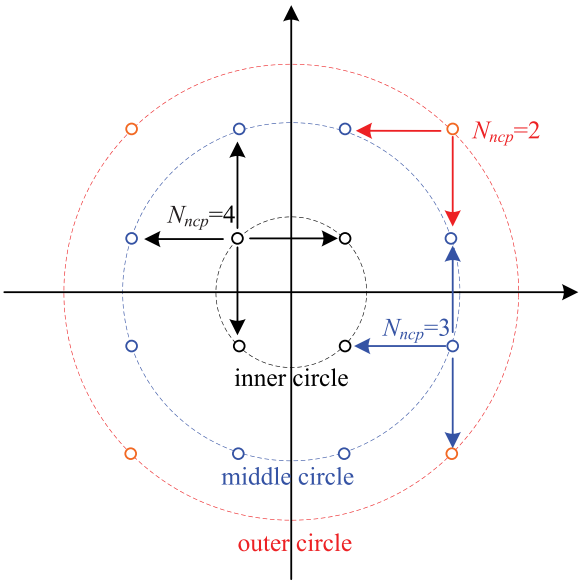

FIGURE 2. 16-QAM signal constellation. It consists of four black points on the inner circle, eight blue points on the middle circle and four red points on the outer circle. The points on the inner, middle, and outer circles have four, three and two nearest neighbors, respectively.

1 in the i-th, $i = 1, 2, \ldots, n$ entry if the i-th subcarrier is active, and 0, otherwise. For example, the AP is $[1\ 1\ 0\ 0]^T$ if $I_\beta = \{1, 2\}$. Then, with the direct extension of the definition in [33], it can be readily shown that the OFDM-IM signal can only move to the signal with the same AP in the LAS search which will limit the performance.

Here, we present a definition of the nearest neighbor, which will admit the signal movement from one AP to another in the LAS search. Given a vector $\mathbf{x} = [\mathbf{x}_1, \mathbf{x}_2, \ldots, \mathbf{x}_u]^T$ consisting of u OFDM-IM blocks, its nearest neighbor can be defined as follows.

1) Only one OFDM-block is different between $\mathbf{x}$ and its neighbor. Denote $\mathbf{x}'_{[\beta]} = [\mathbf{x}_1, \ldots, \mathbf{x}_{\beta-1}, \mathbf{x}'_\beta, \mathbf{x}_{\beta+1}, ..., \mathbf{x}_u]^T$, $\beta = 1, \ldots, u$ as the neighbor with only the β-th IM block being different.
2) For $\mathbf{x}$ and its neighbor $\mathbf{x}'_{[\beta]}$, the IM blocks $\mathbf{x}_\beta$ and $\mathbf{x}'_\beta$ are related as follows. Denote the i-th, $i = 1, \ldots, n$ entry of $\mathbf{x}_\beta$ by $x_{\beta,i}$, i.e, $\mathbf{x}_\beta = \left[x_{\beta,1}, \ldots, x_{\beta,n}\right]^T$. Given $\mathbf{x}_\beta$, $\mathbf{x}'_\beta$ can be divided into two classes.

In the first class, $\mathbf{x}'_\beta$ differs from $\mathbf{x}_\beta$ in only one non-zero entry. Recall I_β is the set of the indices of non-zero entries in $\mathbf{x}_\beta$. Assume $\mathbf{x}'_\beta$ differs from $\mathbf{x}_\beta$ in the $i_{\beta,t}$-th position. Then, $x'_{\beta,i_{\beta,t}}$ should be the nearest constellation point from $x_{\beta,i_{\beta,t}}$. Denote $N_{ncp}\left(x_{\beta,i_{\beta,t}}\right)$ as the number of the nearest constellation points from $x_{\beta,i_{\beta,t}}$. In general, $N_{ncp}\left(x_{\beta,i_{\beta,t}}\right)$ is different for different constellation points. For example, for the 16-QAM constellation consisting of three circles shown in Fig. 2, $N_{ncp} = 4$, 3, and 2 for the constellation points on the inner, middle, and outer circles, respectively. Specifically, when all the points in the signal constellation are geometrically uniform, N_{ncp} will be the same for all the signal points. For example, for the QPSK constellation, $N_{ncp} = 2$ for all the signal points. Denote $\bar{N}_{ncp}$ as the averaged N_{ncp}. Then, the $\mathbf{x}'_\beta$ in this class has $n_a\bar{N}_{ncp}$ candidates.

Example 2: Assume $n = 4$, $n_a = 2$, 16-QAM modulation, and $\mathbf{x}_\beta = 1/\sqrt{10}[1 + j, -1 + 3j, 0, 0]^T$. Note that the nearest signal points of $1 + j$ are $-1 + j$, $3 + j$, $1 - j$, and $1 + 3j$, and those of $-1 + 3j$ are $-3 + 3j$, $1 + 3j$, and $-1 + j$. The nearest neighbors of $\mathbf{x}_\beta$ belonging to the first class are shown at the bottom of this page.

In the second class, $\mathbf{x}'_\beta$ differs from $\mathbf{x}_\beta$ with a Hamming distance of 2, i.e., from $\mathbf{x}_\beta$ to $\mathbf{x}'_\beta$, one non-zero entry of $\mathbf{x}_\beta$ becomes zero and one zero entry become a least-energy signal point of the constellation employed. Moreover, the new $\mathbf{x}'_\beta$ should be also a legitimate IM block. Denote N_{le} as the number of the least-energy signal points of the constellation, and N_{HD2} as the number of the legitimate APs which has a

$$\mathbf{x}'_\beta \in 1/\sqrt{10}\left\{\begin{bmatrix}-1+j\\-1+3j\\0\\0\end{bmatrix}, \begin{bmatrix}3+j\\-1+3j\\0\\0\end{bmatrix}, \begin{bmatrix}1-j\\-1+3j\\0\\0\end{bmatrix}, \begin{bmatrix}1+3j\\-1+3j\\0\\0\end{bmatrix}, \begin{bmatrix}1+j\\-3+3j\\0\\0\end{bmatrix}, \begin{bmatrix}1+j\\1+3j\\0\\0\end{bmatrix}, \begin{bmatrix}1+j\\-1+j\\0\\0\end{bmatrix}\right\}$$

Hamming distance 2 with the AP of $\mathbf{x}_\beta$. Then, $\mathbf{x}'_\beta$ in this form has $N_{HD2}N_{le}$ candidates.

Example 2 (continued): Assume the legitimate APs are those associated with $I_\beta \in \{\{1,2\},\{2,3\},\{3,4\},\{4,1\}\}$. Given $\mathbf{x}_\beta$ in Example 1, it has $I_\beta(\mathbf{x}_\beta) = \{1,2\}$. Obviously, N_{HD2} =2, and $I_\beta(\mathbf{x}'_\beta) \in \{\{2,3\},\{4,1\}\}$. Noting that the least energy points are $1+j$, $-1+j$, $1-j$, and $-1-j$, $\mathbf{x}'_\beta$ in this class belongs to the equation shown at the bottom of the next page.

According to the above definition, for one OFDM-IM signal $\mathbf{x}$, the number of the nearest neighbors is $N_{nb} = u\left(n_a\bar{N}_{ncp} + N_{HD2}N_{le}\right)$. Given the definition of the nearest neighbors, the LAS detector in [33] can be employed here by a direct extension. For autonomy, the LAS is summarized as Algorithm II. In line 3 of Algorithm II, N_{iter_max} denotes the number of maximum iterations. In line 6, as shown in [33], the metric Γ' can be efficiently computed by utilizing the fact that the difference vector $\mathbf{x}_{[\beta]} - \mathbf{x}'_{[\beta]}$ has only one (neighbor vector belongs to the first class) or two (second class) non-zero entries, and the complexity in terms of the number of complex multiplications is $\mathcal{O}(NN_{hw})$ with N_{hw}, $1 < N_{hw} < 2$ being the average Hamming weight of the difference vector. Therefore, the complexity of LAS is $\mathcal{O}(NN_{hw}N_{nb}N_{iter})$ without taking into account the computation cost of the initial estimation, where N_{iter} is the average number of iterations in the practical implementation.

Algorithm 2 LAS Detector

Input: $\mathbf{y}, \mathbf{G}$
Output: $\hat{\mathbf{x}}$
1. Initialization $\hat{\mathbf{x}} = \mathbf{x} = \mathbf{x}^{(0)}$, $\Gamma = \left\|\mathbf{y} - \mathbf{G}\mathbf{x}^{(0)}\right\|^2$
2. Set $t = 1, flag\_c = 0, flag\_m = 0$;
3. **while** ($t <= N_{iter\_max}$&&$flag\_c = 0$)
4. **for** $\beta = 1, \ldots, u$
5. **for** each neighbor $\mathbf{x}'_{[\beta]}$ of $\mathbf{x}$
6. compute the metric $\Gamma' = \left\|\mathbf{y} - \mathbf{G}\mathbf{x}'_{[\beta]}\right\|^2$
7. If $\Gamma' < \Gamma$, set $\hat{\mathbf{x}} = \mathbf{x}'_{[\beta]}$, $\Gamma = \Gamma'$, and $flag\_m = 1$.
8. **end for**
9. **end for**
10. set $\mathbf{x} = \hat{\mathbf{x}}$
11. if $flag\_m = 0$, then set $flag\_c = 1$
12. $t = t + 1$
13. **end while**

Example 3: With the same parameter settings as Example 2, it can be readily shown that there are 6 and 8 neighbor vectors in the first and second class, respectively, and $\bar{N}_{ncp} = 3, N_{HD2} = 2, N_{hw} = (6\times 1 + 8\times 2)/14 = 1.57$, $N_{nb} = 14u$. When QPSK modulation is considered, it has 4 and 8 neighbor vectors in the first and second class, respectively, and $\bar{N}_{ncp} = 2, N_{HD2} = 2, N_{hw} = (4\times 1+8\times 2)/12 = 1.67, N_{nb} = 12u$.

The initial estimation $\mathbf{x}^{(0)}$ should be the solution from some low-complexity detectors, e.g., the SIC-SDR and SP detectors. Furthermore, multiple-restart LAS detector with multiple initial estimations can also be utilized, where multiple LAS detector with different initial estimations are performed in parallel and the best solution as the final estimation. For notation simplicity, the LAS detector with the initial estimation from the SIC-SDR detector is abbreviated as LAS with SIC-SDR. Similarly, the notation LAS with SP is defined. The 2-restart LAS detector with initial estimations from SP and SIC-SDR, shown in Fig. 1(*b*), is abbreviated as LAS with SP & SIC-SDR. The complexities of these combined detectors in terms of the number of complex multiplications are listed in Table 1.

TABLE 1. Complexity orders of the proposed detectors.

Detector	Complexity Order
SDR	$N^{3.5}$
SIC-SDR	$K(N/K)^{3.5}$
SP	$Nn2^p$
MMSE-LLR	N^3
LAS with SP	$Nn2^p + NN_{hw}N_{nb}N_{iter}$
LAS with SIC-SDR	$K(N/K)^{3.5} + NN_{hw}N_{nb}N_{iter}$
LAS with SP & SIC-SDR	$Nn2^p + K(N/K)^{3.5} + NN_{hw}N_{nb}N_{iter}$

V. SIMULATION RESULTS

In this section, the simulation results are given to evaluate the performance of the proposed detector. The Rayleigh fading channel is assumed. The Jakes model [36] is used to generate the RTV fading channel with the normalized Doppler frequency $f_dT_s = 0.15$. The exponential power-delay profile is considered, i.e., the variance of the v-th channel tap is $\sigma_v^2 \propto \exp(-v/V)$. The numbers of subcarriers in one OFDM symbol and one IM block are $N = 96$ and $n = 4$, respectively, and the number of active subcarriers in one IM block is $n_a = 2$. The CP length and the number of channel taps are $L = V = 10$. The transmit signal-to-noise ratio (SNR) is defined as $E_b/N_{0,T}$ where $E_b = (N+L)/B$ is the averaged transmit energy per bit and $N_{0,T} = nN_{0,F}/n_a$ is the noise variance in the time domain.

In the SDR and SIC-SDR detectors, the number of candidate vectors L_r in the randomization procedure is set to be 16 for QPSK modulation and 64 for 16-QAM modulation. In the SIC-SDR detector, the number of groups is set to be 6, i.e. $K = 6$. In the combined detectors, the number of maximum iterations in LAS algorithm is set to be $N_{iter\_max} = 100$.

In Figs. 3 and 4, the BER performance of the proposed detectors is given with QPSK and 16-QAM modulations, respectively. As a reference, the BER curves of the SP and MMSE-LLR detectors [3] are also presented.

From both figures, first, the error floor can be observed in all the detectors except the proposed SDR detector and

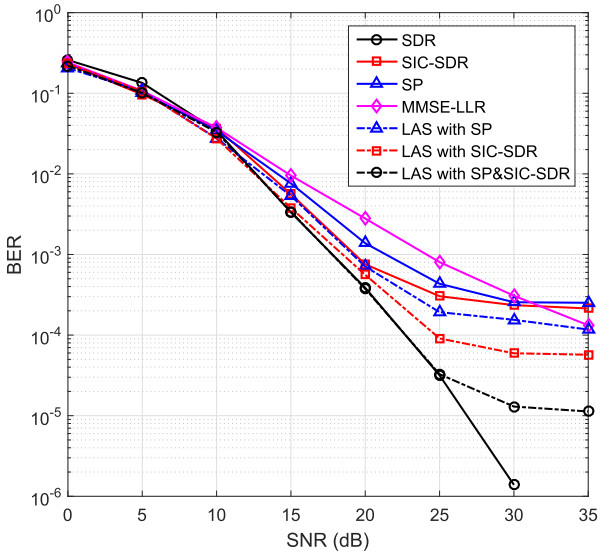

FIGURE 3. Simulated BER performance of various detectors with QPSK modulation.

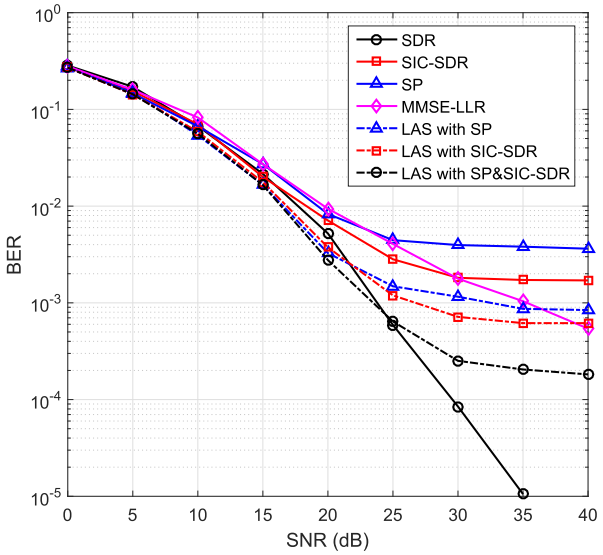

FIGURE 4. Simulated BER performance of various detectors with 16-QAM modulation.

the MMSE-LLR detector. This can be interpreted by the fact that both the SDR and MMSE-LLR detectors process all the subcarreirs in one OFDM symbol simultaneously and thereby no error propagation exists, while the other detectors employ the SIC strategy which will suffer from the error propagation.

Second, the SDR detector has the best performance in the high SNR region in all the detectors considered here. The cost is the highest polynomial complexity from Table 1. Therefore, the SDR detector is a good candidate when the number N of the subcarriers is small-to-medium.

Third, the SIC-SDR detector suffers from a severe performance degradation compared with the SDR detector due to the error propagation, although a large complexity reduction is achieved from Table 1. Fourth, in general, the SIC-SDR detector has some performance gain over the SP detector with comparable complexity. For example, from Table 1, the complexity orders of the SIC-SDR and SP detectors are $K(N/K)^{3.5} = 6 \times 16^{3.5} = 98304$ and $Nn2^p = 96 \times 4 \times 2^6 = 24576$, respectively, for QPSK modulation, and the numbers are 98304 and $Nn2^p = 96 \times 4 \times 2^{10} = 393216$, respectively, for 16-QAM modulation. On the other hand, from Figs. 3 and 4, a lower error floor is achieved in the SIC-SDR detector compared with the SP detector.

Fifth, the post-processing by the LAS algorithm can achieve a large performance improvement. For example, from all the figures, the LAS with SIC-SDR achieves a large performance gain over the SIC-SDR detector. In Fig. 3, the error floor appears at BER=2×10^{-4} in the SIC-SDR detector while at BER=6×10^{-5} in the LAS with SIC-SDR detector. Moreover, the 2-restart LAS with SP & SIC-SDR detector has a larger performance improvement than both the one-restart LAS with SP and LAS with SIC-SDR detectors.

Finally, in the case with small signal constellation (QPSK), the LAS with SP & SIC-SDR detector shows nearly the same performance as the SDR detector untill BER=3×10^{-5} (SNR smaller than 25dB) from Fig. 3. On the other hand, Fig. 5 gives the average number of iterations of LAS algorithm in the combined detectors. From this figure, the practical iteration number is usually much smaller than the maximum iteration number N_{iter_max} especially in the high SNR region. For example, at SNR larger than 20dB, the average number of iterations is only a little larger than one ($N_{iter} = 1.069$, 1.036, 1.027, and 1.023 for SNR=20, 25, 30, and 35dB, respectively) in the LAS with SIC-SDR detector, which means that, in most case, only the nearest neighbors of the initial estimation are searched in the LAS

$$\mathbf{x}'_\beta \in 1/\sqrt{10} \left\{ \begin{bmatrix} 0 \\ -1+3j \\ 1+j \\ 0 \end{bmatrix}, \begin{bmatrix} 0 \\ -1+3j \\ 1-j \\ 0 \end{bmatrix}, \begin{bmatrix} 0 \\ -1+3j \\ -1+j \\ 0 \end{bmatrix}, \begin{bmatrix} 0 \\ -1+3j \\ -1-j \\ 0 \end{bmatrix}, \right.$$
$$\left. \begin{bmatrix} 1+j \\ 0 \\ 0 \\ 1+j \end{bmatrix}, \begin{bmatrix} 1+j \\ 0 \\ 0 \\ 1-j \end{bmatrix}, \begin{bmatrix} 1+j \\ 0 \\ 0 \\ -1+j \end{bmatrix}, \begin{bmatrix} 1+j \\ 0 \\ 0 \\ -1-j \end{bmatrix} \right\}$$

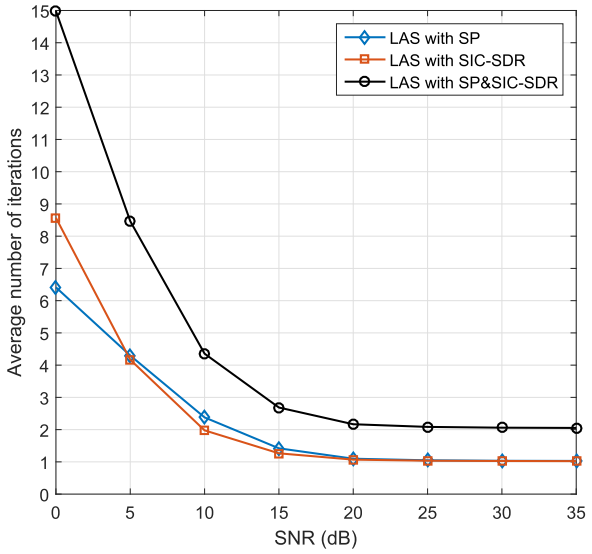

FIGURE 5. Average number of iterations in the LAS algorithm of the combined detectors with QPSK modulation.

algorithm. Furthermore, from Table 1, the complexity order is $N^{3.5} = 96^{3.5} = 8668607$ for the SDR detector, while $Nn2^p + K(N/K)^{3.5} + NN_{hw}N_{nb}N_{iter} \approx 96 \times 4 \times 2^6 + 6 \times 16^{3.5} + 96 \times 1.67 \times 288 \times 2 \approx 215224$ for the LAS-with SP & SIC-SDR detector when the QPSK modulation is employed. Here, $N_{nb} = 12 \times 24 = 288$, $N_{hw} = 1.67$, and $N_{iter} \approx 2$ at SNR larger than 20dB from Fig. 5 are used in the complexity computation of the latter detector. Therefore, in terms of the performance-complexity tradeoff, the combined detectors will be recommended when N is large.

VI. CONCLUSION

In this paper, we studied the application of the SDR-based convex programming to the OFDM-IM detection in the RTV channel. By designing the convex constrains associated with the signal feature of OFDM-IM properly, the proposed SDR detector shows better performance than conventional detectors with a higher polynomial complexity. To reduce the complexity, the ordered SIC strategy was utilized in the SDR detector, and the resulted SIC-SDR detector suffers from error propagation and shows a large performance gap from the SDR detector in the high SNR region. To reduce the gap, the combined LAS and SIC-SDR detector was further proposed, which achieves excellent performance-complexity tradeoff.

REFERENCES

[1] R. Abu-alhiga and H. Haas, "Subcarrier-index modulation OFDM," in *Proc. IEEE Int. Sym. Pers., Indoor, Mobile Radio Commun.*, Tokyo, Japan, Sep. 2009, pp. 177–181.
[2] D. Tsonev, S. Sinanovic, and H. Haas, "Enhanced subcarrier index modulation (SIM) OFDM," in *Proc. IEEE GLOBECOM*, Dec. 2011, pp. 728–732.
[3] E. Başar, Ü. Aygölü, E. Panayirci, and H. V. Poor, "Orthogonal frequency division multiplexing with index modulation," *IEEE Trans. Signal Process.*, vol. 61, no. 22, pp. 5536–5549, Nov. 2013.
[4] E. Başar, Ü. Aygölü, and E. Panayirci, "Orthogonal frequency division multiplexing with index modulation in the presence of high mobility," in *Proc. BlackSeaCom*, 2012, pp. 147–151.
[5] M. Wen, X. Cheng, and L. Yang, "Optimizing the energy efficiency of OFDM with index modulation," in *Proc. IEEE Int. Conf. Commun. Syst.*, Nov. 2014, pp. 31–35.
[6] W. Li, H. Zhao, C. Zhang, L. Zhao, and R. Wang, "Generalized selecting sub-carrier modulation scheme in OFDM system," in *Proc. IEEE ICC Workshops*, Sydney, NSW, Australia, Jun. 2014, pp. 907–911.
[7] Y. Xiao, S. Wang, L. Dan, X. Lei, P. Yang, and W. Xiang, "OFDM with interleaved subcarrier-index modulation," *IEEE Commun. Lett.*, vol. 18, no. 8, pp. 1447–1450, Aug. 2014.
[8] E. Basar, "OFDM with index modulation using coordinate interleaving," *IEEE Wireless Commun. Lett.*, vol. 4, no. 4, pp. 381–384, Aug. 2015.
[9] J. Zheng and R. Chen, "Achieving transmit diversity in OFDM-IM by utilizing multiple signal constellations," *IEEE Access*, vol. 5, pp. 8978–8988, Jun. 2017.
[10] R. Fan, Y. J. Yu, and Y. L. Guan, "Generalization of orthogonal frequency division multiplexing with index modulation," *IEEE Trans. Wireless Commun.*, vol. 14, no. 10, pp. 5350–5359, Oct. 2015.
[11] X. Yang, Z. Zhang, P. Fu, and J. Zhang, "Spectrum-efficient index modulation with improved constellation mapping," in *Proc. HMWC*, Xi'an, China, Oct. 2015, pp. 91–95.
[12] M. Wen, X. Cheng, M. Ma, B. Jiao, and H. V. Poor, "On the achievable rate of OFDM with index modulation," *IEEE Trans. Signal Process.*, vol. 64, no. 8, pp. 1919–1932, Apr. 2016.
[13] Y. Ko, "A tight upper bound on bit error rate of joint OFDM and multi-carrier index keying," *IEEE Commun. Lett.*, vol. 18, no. 10, pp. 1763–1766, Oct. 2014.
[14] B. Zheng, F. Chen, M. Wen, F. Ji, H. Yu, and Y. Liu, "Low complexity ML detector and performance analysis for OFDM with in-phase/quadrature index modulation," *IEEE Commun. Lett.*, vol. 19, no. 11, pp. 1893–1896, Nov. 2015.
[15] T. Mao, Z. Wang, Q. Wang, S. Chen, and L. Honzo, "Dual-mode index modulaton aided OFDM," *IEEE. Access*, vol. 5, pp. 50–60, Feb. 2017.
[16] J. Zheng and H. Lv, "Peak-to-average power ratio reduction in OFDM index modulation through convex programming," *IEEE Commun. Lett.*, vol. 21, no. 7, pp. 1505–1508, Jul. 2017.
[17] J. Zheng, "Adaptive index modulation for parallel Gaussian channels with finite alphabet inputs," *IEEE Trans. Veh. Techol.*, vol. 65, no. 8, pp. 6821–6827, Aug. 2016.
[18] M. Wen, Y. Li, X. Cheng, and L. Yang, "Index modulated OFDM with ICI self-cancellation in underwater acoustic communications," in *Proc. 48th Asilomar Conf. Signals, Syst. Comput*, Pacific Grove, CA, USA, Nov. 2014, pp. 338–342.
[19] M. Wen, X. Cheng, L. Yang, Y. Li, X. Cheng, and F. Ji, "Index modulated OFDM for underwater acoustic communications," *IEEE Commun. Mag.*, vol. 54, no. 5, pp. 132–137, May 2016.
[20] J. Zheng and R. Chen, "Linear processing for intercarrier interference in OFDM index modulation based on capacity maximization," *IEEE Signal Process. Lett.*, vol. 24, no. 5, pp. 683–687, May 2017.
[21] F. Yao, J. Zheng, and Z. Li, "MIMO OFDM index modulation with circular-shift-based activation pattern for rapidly time-varying channels," in *Proc. IEEE VTC-Spring HMWC*, Nanjing, China, May 2016, pp. 1–4.
[22] E. Başar, "Multiple-input multiple-output OFDM with index modulation," *IEEE Signal Process. Lett.*, vol. 22, no. 12, pp. 2259–2263, Dec. 2015.
[23] E. Basar, "On multiple-input multiple-output OFDM with index modulation for next generation wireless networks," *IEEE Trans. Signal Process.*, vol. 64, no. 15, pp. 3868–3878, Aug. 2016.
[24] T. Datta, H. S. Eshwaraiah, and A. Chockalingam, "Generalized space-and-frequency index modulation," *IEEE Trans. Veh. Technol.*, vol. 65, no. 7, pp. 4911–4924, Jul. 2016.
[25] N. Ishikawa, S. Sugiura, and L. Hanzo, "Subcarrier-index modulation aided OFDM-will it work?" *IEEE Access*, vol. 4, pp. 2580–2593, 2016.
[26] E. Basar, "Index modulation techniques for 5G wireless network," *IEEE Commun. Mag.*, vol. 54, no. 7, pp. 168–175, Jul. 2016.
[27] D. P. Palomar and Y. C. Eldar, Ed., *Convex Optimization in Signal Processing and Communications*. Cambridge, U.K.: Cambridge Univ. Press, 2010.
[28] Y. Yang, C. Zhao, P. Zhou, and W. Xu, "MIMO detection of 16-QAM signaling based on semidefinite relaxation," *IEEE Signal Process. Lett.*, vol. 14, no. 11, pp. 797–800, Nov. 2007.

[29] N. D. Sidiropoulos and Z. Luo, "A semidifinite relaxation approach to MIMO detection for high-order QAM constellations," *IEEE Signal Process. Lett.*, vol. 13, no. 9, pp. 525–528, Sep. 2006.
[30] A. Mobasher, M. Taherzadeh, R. Sotirov, and A. M. Khandani, "A near-maximum-likelihood decoding algorithm for MIMO systems based on semi-definite programming," *IEEE Trans. Inf. Theorey*, vol. 53, no. 11, pp. 3869–3886, Nov. 2007.
[31] A. Wissel, Y. C. Eldar, and S. Shamai (Shitz), "Semidefinite relaxation for detection of 16-QAM signaling," *IEEE Signal Process. Lett.*, vol. 12, no. 9, pp. 653–656, Sep. 2005.
[32] M. Kisialiou, X. Luo, and Z. Luo, "Efficient implementation of quais-maixmum-likelihood detection based on semidefinite relaxation," *IEEE Trans. Signal Process.*, vol. 57, no. 12, pp. 4811–4822, Sep. 2009.
[33] K. V. Vardhan, S. K. Mohammed, A. Chockalingam, and B. S. Rajan, "A low-compelxity detector for large MIMO systems and multicarrier CDMA systems," *IEEE J. Sel. Areas Commun.*, vol. 26, no. 3, pp. 473–485, Apr. 2008.
[34] M. Grant and S. Boyd. (Sep. 2013). *CVX: MATLAB Software for Disciplined Convex Programming, Version 2.0 Beta*. [Online]. Available: https://www.cvxr.com/cvx
[35] M. C. Grant and S. P. Boyd, "Graph implementations for nonsmooth convex programs," in *Recent Advances in Learning and Control*(Lecture Notes in Control and Information Sciences), V. Blondel, S. P. Boyd, and H. Kimura, Eds. London, U.K.: Springer, 2008, pp. 95–110. [Online]. Available: http://stanford.edu/ boyd/graphdcp
[36] Y. R. Zheng and C. Xiao, "Improved models for the generation of multiple uncorrelated Rayleigh fading waveforms," *IEEE Commun. Lett.*, vol. 6, no. 6, pp. 256–258, Jun. 2002.

JIANPING ZHENG received the B.S., M.S., and Ph.D. degrees in information and communication engineering from Xidian University in 2003, 2006, and 2008, respectively. From 2010 to 2011, he was a Research Fellow with the PWTC Laboratory, Nanyang Technological University, Singapore. He joined the School of Telecommunications Engineering, Xidian University, in 2006, where he is currently an Associate Professor. His current research interests include MIMO, 5G techniques, and signal processing for wireless communications.

HONGMEI LV received the B.S. degree in electronic information engineering from Northeast Petroleum University in 2015. She is currently pursuing the M.S. degree with the School of Telecommunications Engineering, Xidian University. Her research interests include OFDM and 5G techniques.